Targeted Inactivation of Kinesin-1 in Pancreatic β-Cells In Vivo Leads to Insulin Secretory Deficiency

Ju Cui,[1] Zai Wang,[1] Qianni Cheng,[2] Raozhou Lin,[1] Xin-Mei Zhang,[1] Po Sing Leung,[2] Neal G. Copeland,[3] Nancy A. Jenkins,[3] Kwok-Ming Yao,[1] and Jian-Dong Huang[1]

OBJECTIVE—Suppression of Kinesin-1 by antisense oligonucleotides, or overexpression of dominant-negative acting kinesin heavy chain, has been reported to affect the sustained phase of glucose-stimulated insulin secretion in β-cells in vitro. In this study, we examined the in vivo physiological role of Kinesin-1 in β-cell development and function.

RESEARCH DESIGN AND METHODS—A Cre-LoxP strategy was used to generate conditional knockout mice in which the *Kif5b* gene is specifically inactivated in pancreatic β-cells. Physiological and histological analyses were carried out in *Kif5b* knockout mice as well as littermate controls.

RESULTS—Mice with β-cell specific deletion of *Kif5b* (*Kif5b*$^{fl/-}$*:RIP2-Cre*) displayed significantly retarded growth as well as slight hyperglycemia in both nonfasting and 16-h fasting conditions compared with control littermates. In addition, *Kif5b*$^{fl/-}$*:RIP2-Cre* mice displayed significant glucose intolerance, which was not due to insulin resistance but was related to an insulin secretory defect in response to glucose challenge. These defects of β-cell function in mutant mice were not coupled with observable changes in islet morphology, islet cell composition, or β-cell size. However, compared with controls, pancreas of *Kif5b*$^{fl/-}$*:RIP2-Cre* mice exhibited both reduced islet size and increased islet number, concomitant with an increased insulin vesicle density in β-cells.

CONCLUSIONS—In addition to being essential for maintaining glucose homeostasis and regulating β-cell function, Kif5b may be involved in β-cell development by regulating β-cell proliferation and insulin vesicle synthesis. ***Diabetes*** **60:320–330, 2011**

Insulin is exclusively produced and secreted from pancreatic β-cells in two distinct phases in response to elevated blood glucose levels. The first phase of insulin release is triggered by a rapid increase of intracellular calcium level leading to fusion of predocked insulin granules at the plasma membrane (1). The second phase of insulin release requires the mobilization of insulin-containing granules from the storage pool to the β-cell periphery to sustain insulin release (2). The molecular mechanism for the first phase of insulin release has been extensively investigated (1,3–5); however, little is known regarding the second phase of insulin secretion (6).

Pharmacological and cytological observations suggest that dynamic turnover of tubulin and microtubules is important for regulation of intracellular transportation of insulin granules and their subsequent release from β-cells (7). Boyd et al. (8) observed a proportion of insulin-containing vesicles attached along the microtubules by double-immunostaining of primary cultured pancreatic β-cells. Furthermore, colchicine treatment does not affect the immediate release of insulin but significantly attenuates the following sustained phase of response. In addition, Suprenant and Dentler (9) demonstrated direct binding of insulin-containing granules to microtubules in vitro, and that insulin granule movement along microtubules is dependent on microtubule-associated proteins in the presence of ATP. Therefore, it was suggested that microtubules within the β-cell serve as supporting structures (railways) upon which insulin granules travel from the β-cell interior to the plasma membrane.

Kinesin and dynein are two motor proteins that have been identified to translocate cargos along microtubules to opposite directions for fast transportation. Conventional kinesin (Kinesin-1) is a heterotetramer of two heavy chains (KHCs) and two light chains (KLCs). The head domain of KHC contains the ATP binding domain for generating motile force as well as a motif for interaction with microtubules, whereas the tail domain and KLC are responsible for cargo binding (10–12). In mice, three conventional kinesin heavy chain genes have been identified, including *Kif5a*, *Kif5b*, and *Kif5c*. Kif5b is the mouse homologue of the human ubiquitous KHC (13) and was first identified and characterized in pancreatic β-cells (14). The functions and molecular mechanism of kinesin transportation have been extensively studied in neuronal cells and tissues. However, only a few reports are related to the role of this motor protein during cargo transportation in nonneuronal mammalian cell types (15–19). Meng et al. (20) reported that suppression of Kif5b by antisense oligonucleotides inhibits both basal- and glucose-stimulated insulin secretion (GSIS) in primary mouse pancreatic β-cells. Immunocytochemistry study showed that Kif5b is colocalized with some insulin-containing vesicles in β-cell lines (MIN6 & INS-1) (18). Moreover, expression of a dominant-negative KHC motor domain (KHC^{mut}) strongly inhibited the sustained, but not acute, insulin secretion in response to glucose challenge (18). Besides Kif5b, other motor proteins such as myosin Va and dynein are also involved in insulin secretion (21,22).

All the above studies were carried out in an in vitro model, and the physiological role of Kif5b in pancreatic β-cells has not been elucidated in vivo. Therefore, to directly explore the role of Kif5b in β-cells, we generated

From the [1]Department of Biochemistry, Li Ka Shing Faculty of Medicine, The University of Hong Kong, Hong Kong; the [2]Department of Physiology, The Chinese University of Hong Kong, Hong Kong; and the [3]Institute of Molecular and Cell Biology, Agency for Science, Technology and Research, Singapore.

Corresponding author: Jian-Dong Huang, jdhuang@hkucc.hku.hk, or Kwok-Ming Yao, kmyao@hkusua.hku.hk.

Received 26 July 2009 and accepted 20 September 2010. Published ahead of print at http://diabetes.diabetesjournals.org on 24 September 2010. DOI: 10.2337/db09-1078.

a conditional knockout mouse under the control of RIP2-Cre by using a Cre-LoxP recombination system.

RESEARCH DESIGN AND METHODS

Generation of *Kif5b*$^{fl/fl}$ as well as *Kif5b*$^{+/-}$ mice by gene targeting. A bacterial artificial chromosome DNA containing the K*if5b* gene (bacterial artificial chromosome clone 307D12) was partially digested with *Xba*I and subcloned into a pBluescript II-KS plasmid. A plasmid containing a 14.5-kb DNA insert, pBS-*Kif5b*, was identified by Southern blotting using a labeled probe containing exon 2, where the ATP-GTP-A site is located (data not shown). The *TK4* gene from pBS-304 was cloned into the *Sal*I site of pBS-*Kif5b*. The first loxP site was introduced into the first intron of *Kif5b* gene by the recombinogenic targeting of a loxp-Pgk-Tn5-Neo-loxp cassette (PCR amplified from the modified pGK-loxP plasmid with primer: TCTTGT GACTTAGAGTTTATAAAATAGAGTAATTTTGAAAACACATAGATATCTGCAAAC CCTATGCTACTCCGTCG and CGCTCTCCTGAGTAGGACAAATCCGCCGGGACT ATAGGTTGTGTAATGTGTATTTCAAGTCAAAAAATGAATTGAAAAAAA) into pBS-*Kif5b*, followed by removal of the fragment between the two loxP sites via Cre-mediated recombination. The second loxP site accompanying the frt-Pgk-Tn5-Neo-frt cassette was introduced into the second intron of *Kif5b* gene by targeting a frt-Pgk-Tn5-Neo-frt-loxP cassette (PCR amplified from the modified PBS-246-FRT plasmid by PCR primers primer: GGATGCACGGCT GTGAGCACAGGACTTTCCTGTGTTTGGAGT and primer: AGTTGGATTTA AGGAAGTACTACTAAAACTTCAATTAGTCTTACTAAAAA) into the pBS-*Kif5b*-loxP to form the final *Kif5b* knockout construct. The Kif5b-knockout construct, containing 14.5 kb of the *Kif5b* gene, was linearized by NotI and was introduced into CJ7 mouse embryonic cells in Drs. Jenkins and Copeland's lab in National Cancer Institute (NCI), USA, by electroporation and screened by genomic Southern blotting. The neo of *Kif5b* targeted allele was removed by crossing the mice with a Fple deleter strain TgN(ACTFLPe)9205Dym/J (23). *Kif5b*$^{+/-}$ mice were generated by crossing *Kif5b*$^{+/fl}$ mice with actin-Cre mice. Mice with *Kif5b*$^{fl/fl}$ and *Kif5b*$^{+/-}$ genotypes were maintained by backcrossing to C57BL/6N females under a specific pathogen-free environment.

Generation of Kif5b conditional knockout mice and genotyping. RIP2-Cre transgenic mice (24) (from Jackson Laboratory) were first crossed with *Kif5b*$^{+/-}$ to generate *Kif5b*$^{+/-}$*; RIP2-Cre* mice. Then *Kif5b*$^{+/-}$*; RIP2-Cre* were bred with *Kif5b*$^{fl/fl}$ mice to generate the final mutant mice (*Kif5b*$^{fl/-}$*: RIP2-Cre*) as well as their littermates (*Kif5b*$^{+/fl}$, *Kif5b*$^{-/fl}$, and *Kif5b*$^{+/fl}$*:RIP2-Cre*). Genotyping was performed by PCR using corresponding primers. To avoid hormonal effects in physiological assays, only male animals were used in all experiments.

Islet isolation and insulin content measurement. Islet isolation and insulin extraction were carried out as previously described (25). Insulin contents in the islet extracts were analyzed by using the insulin ELISA kit (LINCO Research) and normalized to total protein concentrations determined by Bradford method (Bio-Rad).

Western blot and immunostaining. Protein levels were determined by blotting with anti-Kif5b primary antibody (1:2,000, against synthesized peptide FDKEKANLEAFTADKDIA), anti-Kif5a (1:1,000, against synthesized peptide NGNATDINDNRSDLPC), anti-Kif5c (1:1,000, against synthesized peptide SAK DQKSLEPC), and anti-actin primary antibody (1:3,000, Sigma). Enhanced chemiluminescence kit (Pierce) was used for detection of the immunoreactive bands.

Paraffin sections were immunostained by primary antibodies against Kif5b (1:400), glucagon (1:1,000, Dako), and insulin (1:2,000, Sigma). Visualization of these proteins was realized by incubating with FITC/Cy3 or HRP-conjugated secondary antibodies.

Blood glucose and plasma insulin measurement. Blood was obtained from the tail vein of mice. Blood glucose concentration was determined by Glucometer Elite (Bayor Inc.). Blood samples were collected by Microvette CB300 (Sarstedt) and centrifuged at 5,000 rpm for 5 min at room temperature. After centrifugation, supernatant was collected for determining plasma insulin levels by using insulin ELISA kit (LINCO Research).

Morphometric analysis. Paraffin sections of pancreata were processed for hematoxylin and eosin staining and observed by a light microscope (Carl Zeiss). For transmission electron microscopy (TEM) study, isolated islets were fixed by 2.5% glutaraldehyde in carcodylate buffer and embedded in 2% soft agar, followed by further embedding in fresh epoxy resin. Ultrathin sections were examined on a Philips EM208s transmission electron microscope operated at 80 kV. All photos were analyzed by using Image-Pro Plus software.

Quantitation of β-cell proliferation rates. β-cell division was determined by 5-bromo-2′-deoxyuridine (BrdU) incorporation in 1-month-old mice using BrdU staining kit (ZYMED Laboratory). Pancreatic paraffin sections were further counterstained by hematoxylin and imaged with a Zeiss Axioskop microscope to count BrdU$^+$ β-cells and total nuclei within islets.

Statistical analysis. SigmaStat (Systat Software) was used to analyze all data, which were expressed as mean ± SE. The data were analyzed by one-way ANOVA followed by Tukey test or unpaired two-tailed Student *t* test.

RESULTS

Generation of *Kif5b*$^{fl/-}$*:RIP2-Cre* mice. The ability of RIP2-Cre to induce pancreatic β-cell specific ablation has previously been reported when these founder mice were crossed with mice carrying various floxed genes including glucokinase (26), insulin receptor (27), mitochondrial transcription factor A (28), and hepatocyte growth factor (25). Although RIP2-Cre displays a low level of expression in the hypothalamus, it exhibits high expression level in β-cells within the pancreatic islet (24). Therefore, conditional knockout of *Kif5b* mainly occurred in pancreatic β-cells. Figure 1*A* shows the strategy to generate *Kif5b*$^{fl/fl}$ and *Kif5b*$^{+/-}$ mice. Ablation of one *Kif5b* allele was confirmed by Southern blot as well as Western blot analyses (Fig. 1*B* and *C*). Figure 2*A* shows the genomic organization of different *Kif5b* alleles. P1 and P2 primers were used to differentiate the wild-type and knockout alleles. The distance between P1 and P2 was 6.6 kb in length, which was too long to be amplified by PCR genotyping. Because of the deletion of exon 2, a 219-bp PCR product could be amplified from the *Kif5b* knockout allele accordingly (Fig. 2*B*). P1 and P3 primers, used to differentiate the floxed and wild-type *Kif5b* alleles, result in two bands of 275 and 215 bp, respectively (Fig. 2*B*). The RIP-2 Cre transgene was detected using Cre primers (Fig. 2*B*).

Kif5b was mainly expressed in pancreatic islets (endocrine portion) with little expression in exocrine acinar glands (Fig. 3*A*, left). The positive staining was absent after preincubating the anti-Kif5b antibody with the 18-aa synthesized peptides (Fig. 3*A*, right). To test the efficiency of RIP-2-Cre mediated pancreatic β-cell specific deletion of exon 2 of *Kif5b* allele, we examined the protein expression levels of Kif5a, Kif5b, and Kif5c in hypothalamus and isolated islets from both mutant and wild-type mice (Fig. 3*B*). Inactivation of *Kif5b* by Cre-induced ablation resulted in a reduction of Kif5b protein level in islets, whereas both Kif5a and Kif5c were not detectable in islets although they are highly expressed in hypothalamus, consistent with an earlier finding that their expression is neuronal specific (29). Although RIP2-Cre displayed a low level of expression in the hypothalamus (24), we could not detect significantly decreased Kif5b expression in the hypothalamus due to Cre expression. In contrast, Western blot results showed that Kif5b level in the isolated islets was reduced by at least 80% in mutant mice, compared with the wild-type. Considering the fact that RIP-2 Cre is only expressed in ~80–90% of β-cells and that β-cells account for 75% of islet cells, the Western blot result indicated that Kif5b was absent in most β-cells in the mutant mice islets. The knockout efficiency was further demonstrated by immunohistochemistry analysis of Kif5b expression in pancreatic sections under identical conditions. A significant decrease of Kif5b expression was observed in the islets from mutant mice compared with those in wild-type mice (Fig. 3*C*). Taken together, these results suggested that RIP-2 Cre mediated ablation of exon 2 in *Kif5b* allele had efficiently occurred, leading to significantly reduced Kif5b expression in the islets of mutant mice.

***Kif5b*$^{fl/-}$*:RIP2-Cre* mice have postnatal growth retardation.** Although there was no significant difference in body weight among newborn mice of different genotypes, the mutant mice had progressively reduced growth comparing to

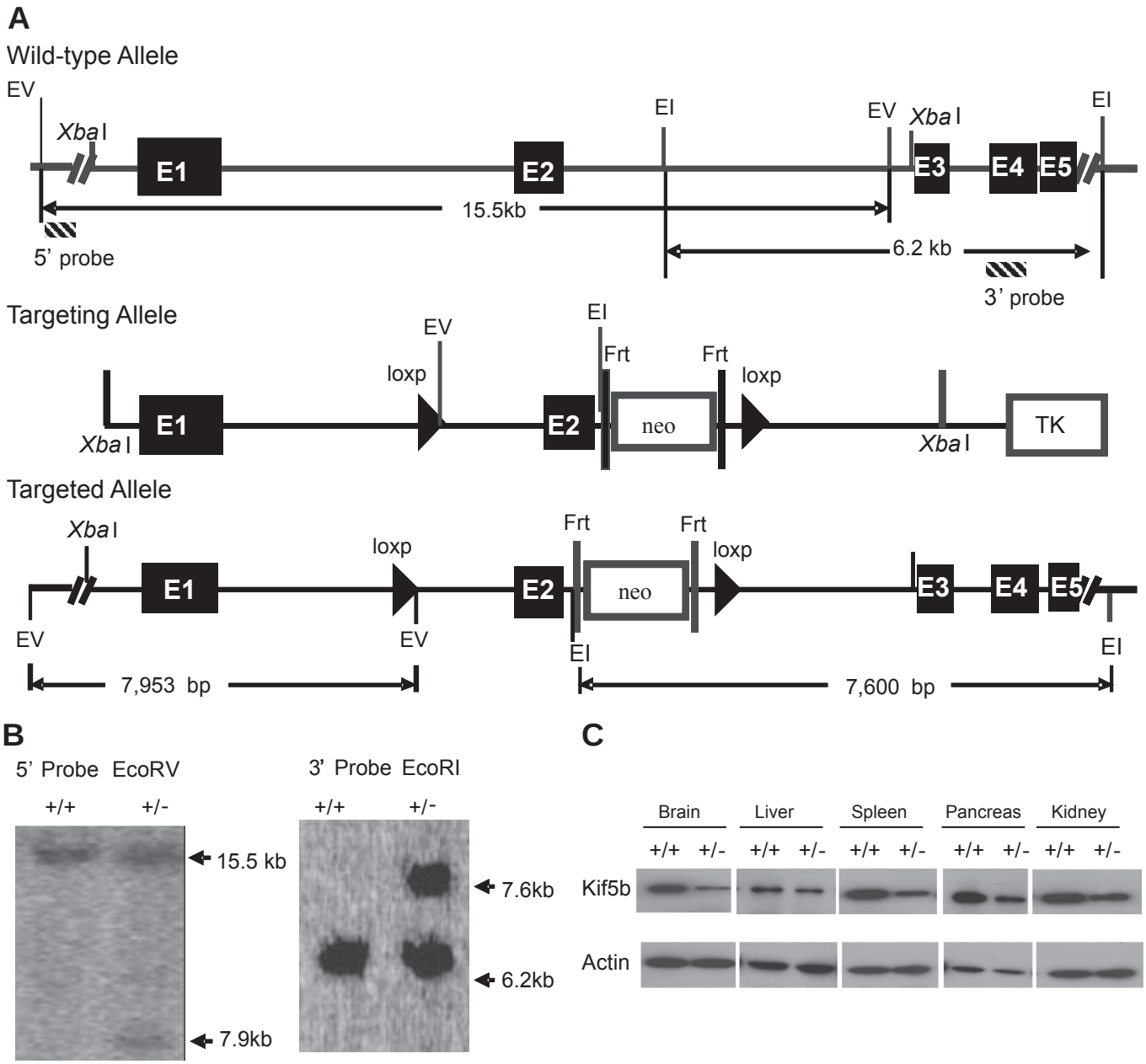

FIG. 1. Targeted disruption of the mouse *Kif5b* gene in ES cells. *A*: Targeting strategy with positive–negative selection. Strategy of genomic Southern blot for screening for the homologous recombinant embryonic stem (ES) cell clones is also included. E1, E2, E3, E4, and E5 represent exon 1, exon 2, exon 3, exon 4, and exon 5 of the *Kif5b* gene, respectively. EI and EV represent *Eco*RI and *Eco*RV cut sites, respectively. The solid square with bars on each side (the bar representing an frt site) represents the 1.7-kb frt-*Neo*^{R}-frt cassette. The triangles represent the LoxP sites (drawing not to scale). Frt: Flippase recognition target; TK: Thymidine Kinase. *B*: Southern blotting analysis of targeted ES clones. Restriction enzyme used for screening 5′ end recombination events was *Eco*RV. A 15.5-kb fragment in wild-type and a 7.9-kb fragment after homologous recombination were expected by the 5′ external probe. Restriction enzyme used for screening 3′ end recombination events was *Eco*RI. A 6.2-kb fragment in wild-type and a 7.6-kb fragment in targeted cells were expected by using the 3′ external probe. These probes are indicated in panel (*A*). *C*: Western blot analysis of Kif5b protein expression in different tissues in homozygous as well as heterozygous mice for the targeted *Kif5b* mutation. Actin was used as internal control.

littermate controls after 3 weeks (Fig. 4*A*). Comparing the mice growth curves, the body weight differences between mutant and control littermates were significant (as shown in the representative photo in Fig. 4*B*) and there was no significant difference among wild-type and heterozygous controls (Fig. 4*A*).

***Kif5b*$^{fl/-}$*:RIP2-Cre* mice develop diabetes due to insulin secretion defect.** To test the effect of Kif5b conditional knockout on glucose homeostasis, we first analyzed the blood glucose level as well as plasma insulin level in both mutant mice and littermate controls. Mutant mice had progressively increased hyperglycemia compared with control littermates in both random (Fig. 4*C*) and 16-h fasting conditions (Fig. 4*D*) within the investigated ages. Therefore, 2- to 3-month-old mice were selected for further study. Consistent with an elevated glucose level, mutant mice had lower plasma insulin concentrations in fasting conditions (Fig. 4*F*) but not in a random fed state (Fig. 4*E*). There were no significant differences in the blood glucose levels as well as plasma insulin concentrations between wild-type and heterozygous controls.

We next assessed the impact of inactivation of *Kif5b* on glucose-regulated insulin secretion in vivo (Fig. 5*A*). The responses of 2- to 3-month-old mutant mice and control

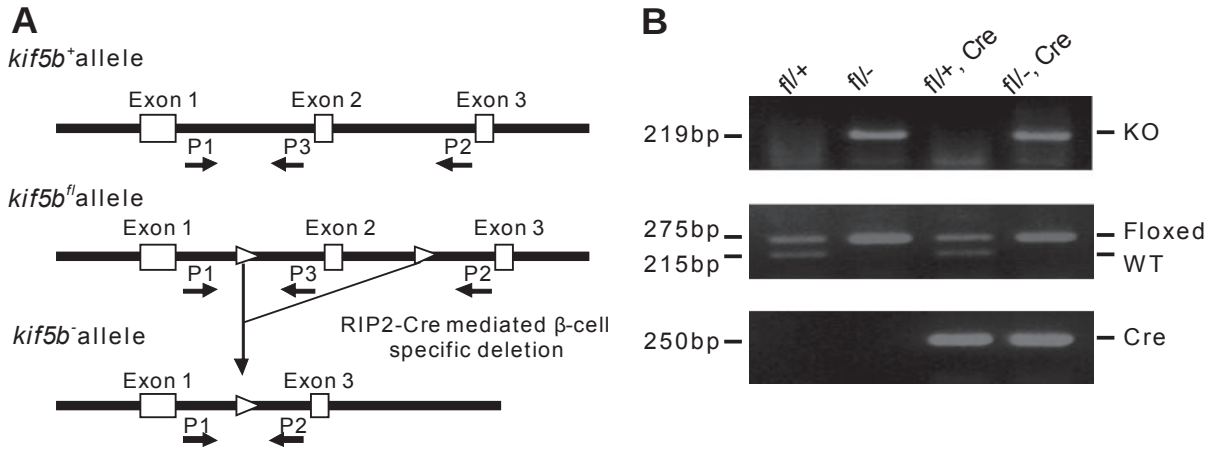

FIG. 2. Assessment of conditional Kif5b inactivation in pancreatic β-cells of *Kif5b$^{fl/-}$:RIP2-Cre* mice. *A*: Schematic illustration of Cre-mediated deletion of exon 2 from the *Kif5b* allele. *B*: Representative pictures show PCR analysis of the offspring genomic DNA from ear. To detect the presence of the floxed *Kif5b* allele, we used primer P1 5′-TGAAGGCTAAGTCAGATATGGATGC-3′ located upstream of loxP site and P3 5′-TTACTAACTGAACCTGGCTTCCTAG-3′ located downstream of loxP site. The presence of *Kif5b* knockout allele was detected by primer P1 5′-TGAAGGCTAAGTCAGATATGGATGC-3′ located in intron 1 and P2 5′-GGATTGGCACCTTTACCTAGAAGG-3′ located in intron 2 of the *Kif5b* gene. The RIP-Cre transgenic mice were identified by amplification of Cre allele using primer 5′-GGACATGTTCAGGGATCGCCAGGCG-3′ and 5′-GGCATGTTCAGGGATCGCCAGGCG-3′. The PCR bands of wild-type (215 bp), floxed (275 bp), null allele (219 bp), and Cre (250 bp) are indicated. Genotypes of representative litters are indicated.

littermates to glucose challenge were examined by performing an intraperitoneal glucose tolerance test (GTT) after 16-h overnight fast. *Kif5b$^{fl/+}$:Cre* mice showed slight glucose intolerance compared with wild-type mice, which may be due to Cre expression in β-cells (30) in addition to the ablation of one *Kif5b* allele. Comparison of the GTT responses between mutant mice and *Kif5b$^{fl/+}$:Cre* mice showed that Kif5b conditional knockout mice had markedly impaired glucose tolerance and this intolerance was not a result of Cre expression. Although the mutant mice had hyperglycemia and glucose intolerance compared with wild-type and *Kif5b$^{fl/+}$:Cre* mice, the blood glucose levels dropped to a similar level as control mice at 15 min after insulin injection (Fig. 5*B*).

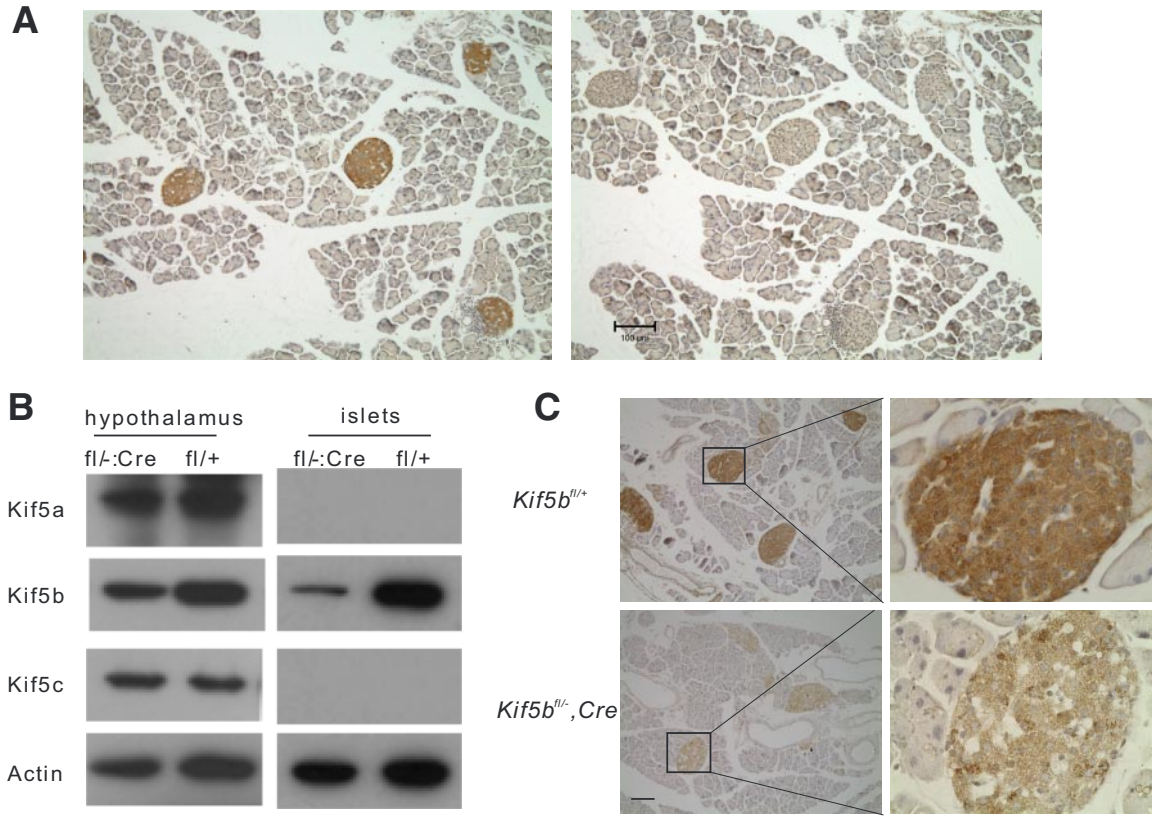

FIG. 3. *A*: Immunohistochemistry analysis of Kif5b expression in wild-type mice pancreas sections (*left*) and antibody specificity test (*right*). *B*: Western blot analysis of Kif5a/Kif5b/Kif5c expression in hypothalamus and isolated islets from mutant and control mice. *C*: Immunohistochemistry analysis of Kif5b expression level in islets from control (*upper*) and mutant mouse (*lower*). (A high-quality color representation of this figure is available in the online issue.)

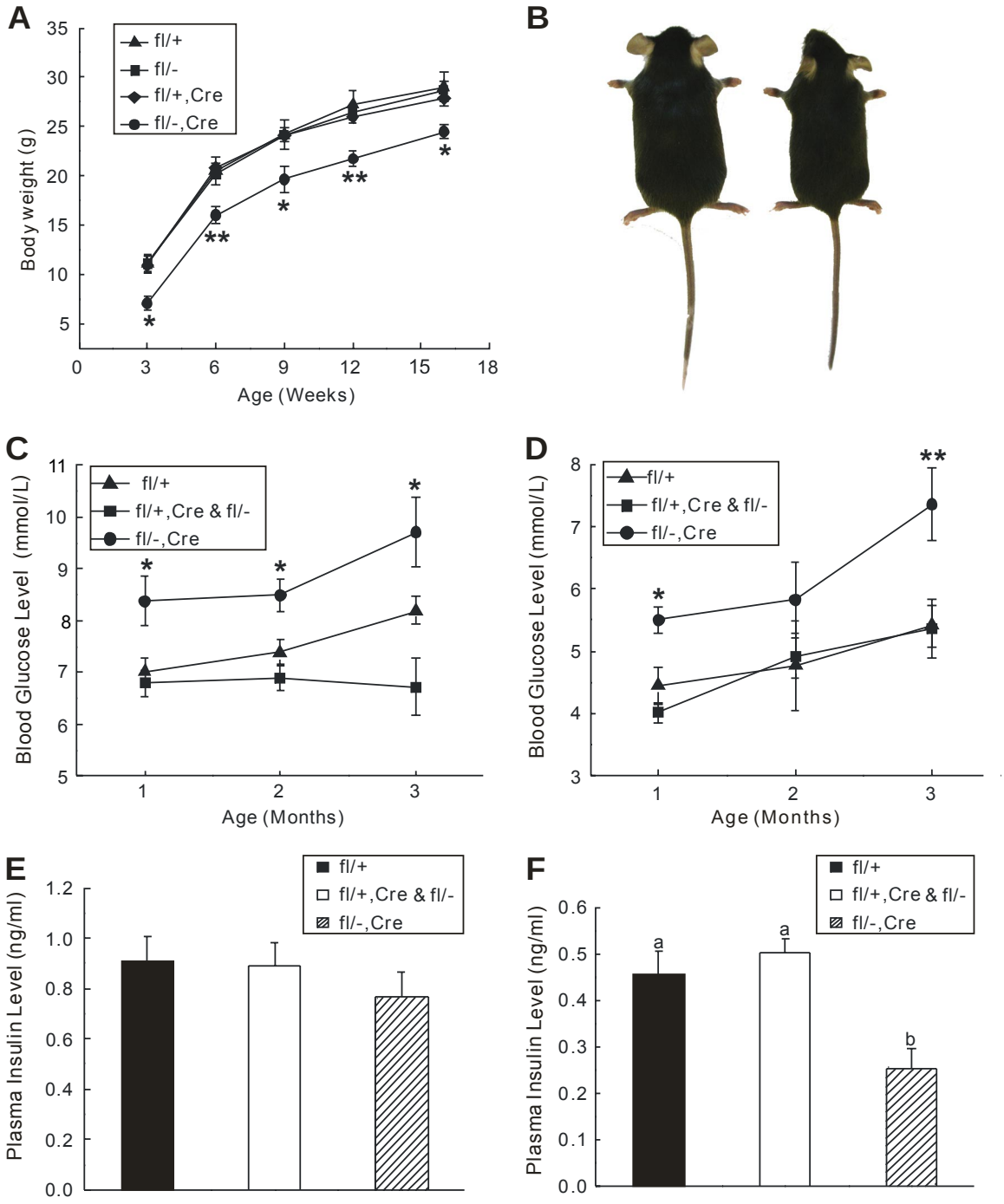

FIG. 4. Physiological features of *Kif5b$^{fl/-}$:RIP2-Cre* mice. *A*: Growth curves of male mice, wild-type (triangle), heterozygous (square), and mutant (circle) mice (n = 6–12). *B*: Photograph of 8-week-old control (*left*) and mutant (*right*) male mice. *C* and *D*: Blood glucose concentrations of male mice with different ages in nonfasting (*C*) and 16-h fasted (*D*) wild-type, heterozygous, and mutant mice (n = 8–22). There is no significant difference of the body weight or blood glucose level between wild-type and heterozygous mice, but these values of mutant mice are significantly different from that of wild-type mice with the same ages. *P < 0.05, **P < 0.01. *E* and *F*: Plasma insulin levels in nonfasting (*E*) and 16-h fasted (*F*) wild-type (black bar), heterozygous (white bar), and mutant mice (striped bar) (n = 6 mice, 2- to 3-month-old). Different letters indicate statistical difference (P < 0.05). The plasma insulin levels in wild-type and heterozygous mice are not different from each other while they are statistically different from that of the mutant mice.

To evaluate the effect of Kif5b deletion on β-cell function, insulin secretion in response to high glucose challenge was examined in 2- to 3-month old mice (Fig. 5*C*). In wild-type mice, insulin secretion was increased by about twofold at 2.5 min after intraperitoneal injection of glucose, reaching a peak at about 5 min, and remained higher than base level for at least 1 h. Glucose tolerance and insulin release were slightly impaired in *Kif5b$^{fl/+}$:Cre* mice compared with wild-type mice in the first 30 min after glucose injection, but the glucose and insulin levels were similar in both genotype mice by 60 min. However, both the early and slow phase of insulin secretion were impaired in *Kif5b$^{fl/-}$:Cre* mice. These results indicated that glucose intolerance in Kif5b conditional knockout mice was not associated with insulin resistance (Fig. 5*B*) but was related to an insulin secretory defect in response to

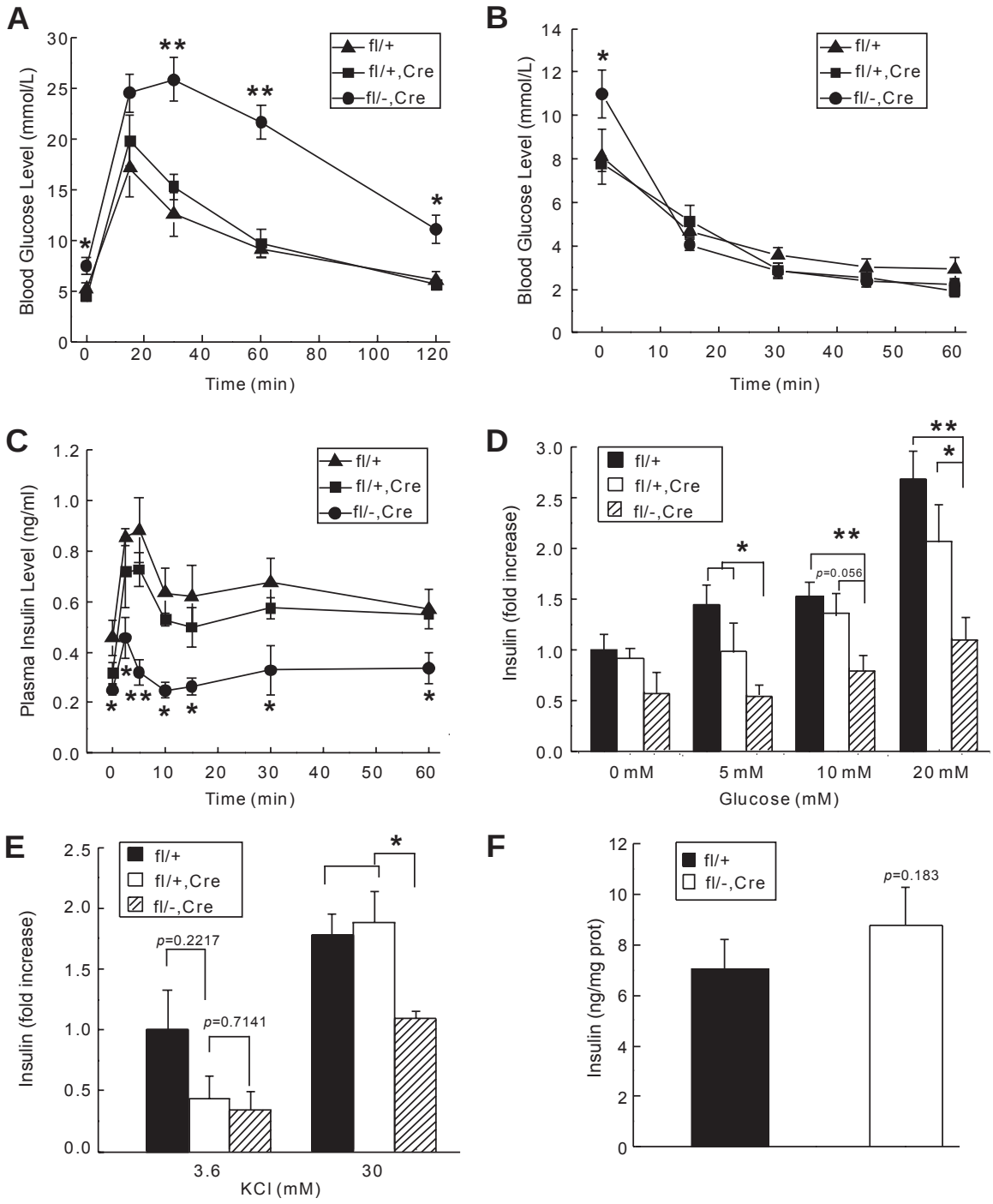

FIG. 5. Effect of Kif5b deletion on glucose metabolism. *A*: Intraperitoneal (i.p.) GTTs were performed on overnight-fasted wild-type (triangle), heterozygous (square), and mutant mice (circle). After overnight fasting, mice were injected with glucose (2 g/kg body wt i.p.) and blood glucose levels were monitored immediately before and 15, 30, 60, and 120 min after glucose injection (n = 5–6 mice per group, 2- to 3-month-old). Mutant mice exhibited reduced glucose tolerance compared with wild-type control, as revealed by significantly increased blood glucose concentrations at corresponding time points (*P < 0.05, **P < 0.01). The glucose tolerance ability was not significantly affected by half reduction of Kif5b expression, because there is no difference for the blood glucose level between control and heterozygous mice. *B*: Insulin sensitivity test was performed on random-fed mice (n = 5–8 mice per group, 2- to 3-month-old). Blood glucose level was measured at the time points indicated before and after intraperitoneal injection of human regular insulin (0.75 units/kg body wt). Although the blood glucose level is high in mutant mice before insulin administration, there is no difference of the glucose level after insulin intraperitoneal injection among the three genotype mice. *C*: GSIS was carried out on overnight-fasted mice as well as isolated islets. Glucose (3 g/kg) was administrated intraperitoneally to overnight (16-h) fasted mice (n = 5 mice per group, 2- to 3-month-old). Plasma insulin levels were measured at indicated time points. GSIS was significantly diminished by Kif5b knockout. *D*: In vitro GSIS was carried out on groups of 10 islets of similar sizes obtained from wild-type (black bar), heterozygous (white bar), and mutant (striped bar) mice and incubated in Krebs-Ringer bicarbonate buffer, supplemented with 10% FBS for 30 min with different glucose concentrations. Experiments were performed in duplicate, and insulin levels were determined by ELISA (n = 4–5 groups for each genotype). Significant decreases in GSIS were observed in mutant mice islets incubated at 5, 10, and 20 mmol/l glucose compared with wild-type mice at the same glucose concentration, and there was no difference between wild-type and heterozygous mice under any glucose concentration. *E*: Insulin release response to indicated concentrations of KCl treatment (n = 3–4 groups for each genotype). Mutant islets exhibit reduced insulin secretion under the stimulation of high concentration of K^+. *F*: Islet insulin content from control (black bar) and mutant islets (white bar) (n = 5 mice per group). P values are indicated in the figure. *P < 0.05, **P < 0.01.

glucose challenge (Fig. 5*C*). It is possible that impaired insulin secretion could be secondary, particularly when considering the expression of Cre in hypothalamic or pituitary cells. To address this possibility, we studied GSIS in isolated islets from mice with different genotypes (Fig. 5*D*). As expected, mutant islets secreted significantly less insulin than control islets under glucose-stimulated conditions. No significant difference in insulin secretion was observed in the absence of glucose. Furthermore, the insulin-secretion defect was progressively enhanced in mutant islets with an increase in glucose concentration. A high level of KCl is known to trigger insulin secretion by inducing plasma membrane depolarization followed by Ca^{2+} influx (1). To further investigate the effect of Kif5b knockout on insulin secretion, KCl-stimulated insulin release from islets was analyzed by 30 mmol/l KCl treatment (Fig. 5*E*). The wild-type islets exhibited stronger secretory responses than mutant islets.

To rule out the possibility that insulin is produced at a lower level in the mutant islet than in the wild-type, an immunostaining assay was carried out. The result demonstrated that the insulin level in mutant mouse was not less than that of wild-type control (Fig. 6*A*). A quantitative analysis of islet insulin content was carried out by ELISA to confirm the result. Results indicated that more insulin accumulated in mutant islets compared with wild-type, although the difference was not statistically significant (Fig. 5*F*). Taken together, it is most likely that the impaired insulin secretion in mutant mice is due to a primary defect in β-cell function.

Pancreas of *Kif5b$^{fl/-}$:RIP2-Cre* mice display decreased islet size. Islets from mutant mice showed similar cellular arrangements and compositions as wild-type mice, with the majority of cells being β-cells and with glucagon-positive α-cells in the periphery region (Fig. 6*A*). There were no significant differences of α- and β-cell ratio between mutant and wild-type islets (Fig. 6*B*). Because Kif5b has been reported to transport insulin vesicles in β-cell lines (MIN6 & INS-1) (18) and mitochondria in neurons (31), we further analyzed the distribution of these vesicles/organelles in mutant and wild-type β-cells by TEM studies (Fig. 7). Compared with the control, mitochondria in mutant β-cells were found to be more likely to cluster in the perinuclear region (Fig. 7*A*). Further quantitative analysis of the distribution of mitochondria in β-cells confirmed that 70% of mitochondria were closer to the nuclear membrane than to the plasma membrane after Kif5b knockout whereas mitochondria in wild-type β-cells were evenly distributed in the cells (Fig. 7*B*). This is consistent with earlier findings that Kif5b is involved in mitochondria translocation (32).

The subcellular localization of insulin vesicles was then analyzed and found to not be affected significantly by the decreased Kif5b level. The cytoplasm of both wild-type and mutant β-cells were filled with insulin vesicles. Insulin vesicle numbers per square μm were determined by counting all insulin vesicles in randomly photographed β-cells (Fig. 7*C*). More insulin granules were found in Kif5b knockout β-cells compared with control cells. This phenomenon is consistent with the observation that insulin secretion by β-cells is affected. Interestingly, a number of small islets were observed in mutant mice as shown in the representative microphotographs in Figure 8*A*. Quantitation of the islet number and size confirmed that the average size of the islet in mutants was smaller than that of the wild-type mice (Fig. 8*B*). However, the total islet mass

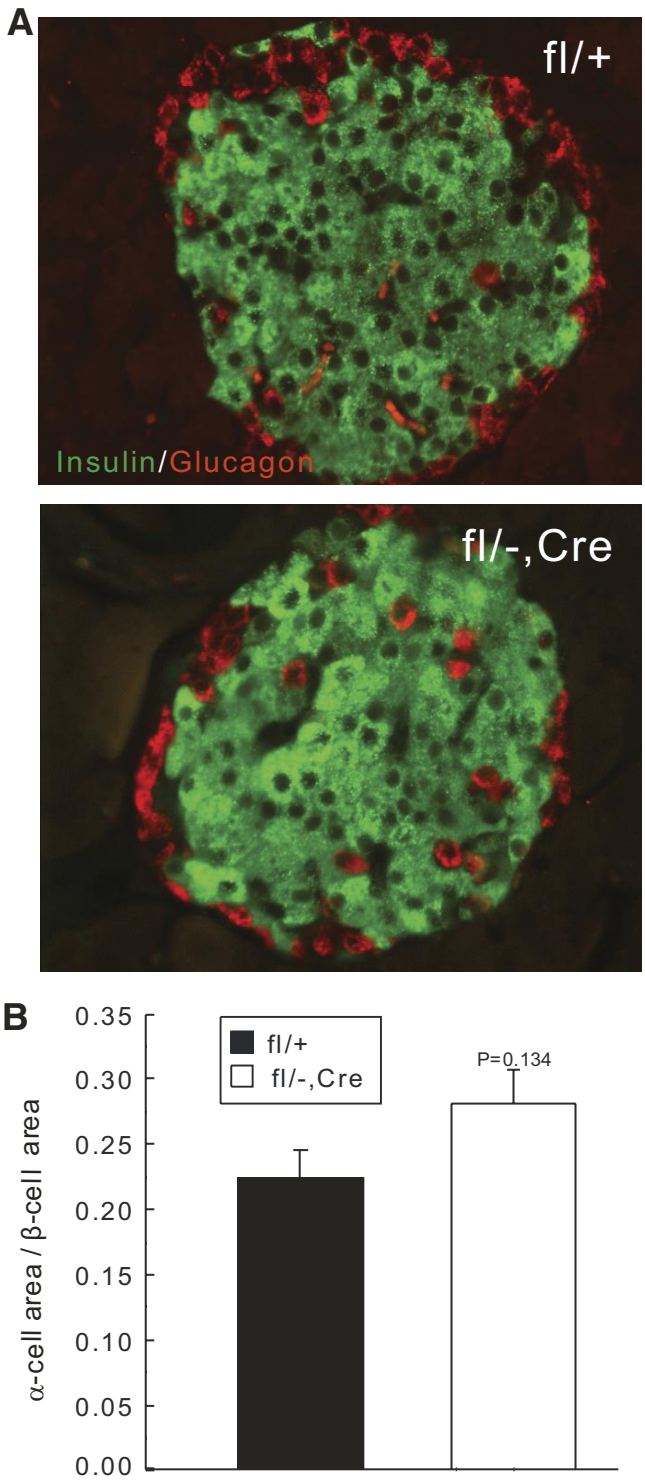

FIG. 6. *Kif5b$^{fl/-}$:RIP2-Cre* mice had normal islet morphology, islet cell composition, and β-cell size. A slight increase in islet insulin content was observed. *A*: Immunofluorescence staining for insulin (green) and glucagon (red) in control (*upper*) and mutant mice (*lower*) (2- to 3-month-old). *B*: Statistical analysis of α- and β-cell ratio in control (black bar) and mutant (white bar) mice (n = 3 mice per group); immunofluorescent staining was carried out on two sections (>300 μm apart) for α-cell (red) and β-cell (green), and all islets on the sections were imaged. (A high-quality color representation of this figure is available in the online issue.)

was not decreased in Kif5b deficient mice (Fig. 8*C*), concomitant with an increase of islet number (Fig. 8*D*). Histomorphometric analysis of the size and number of

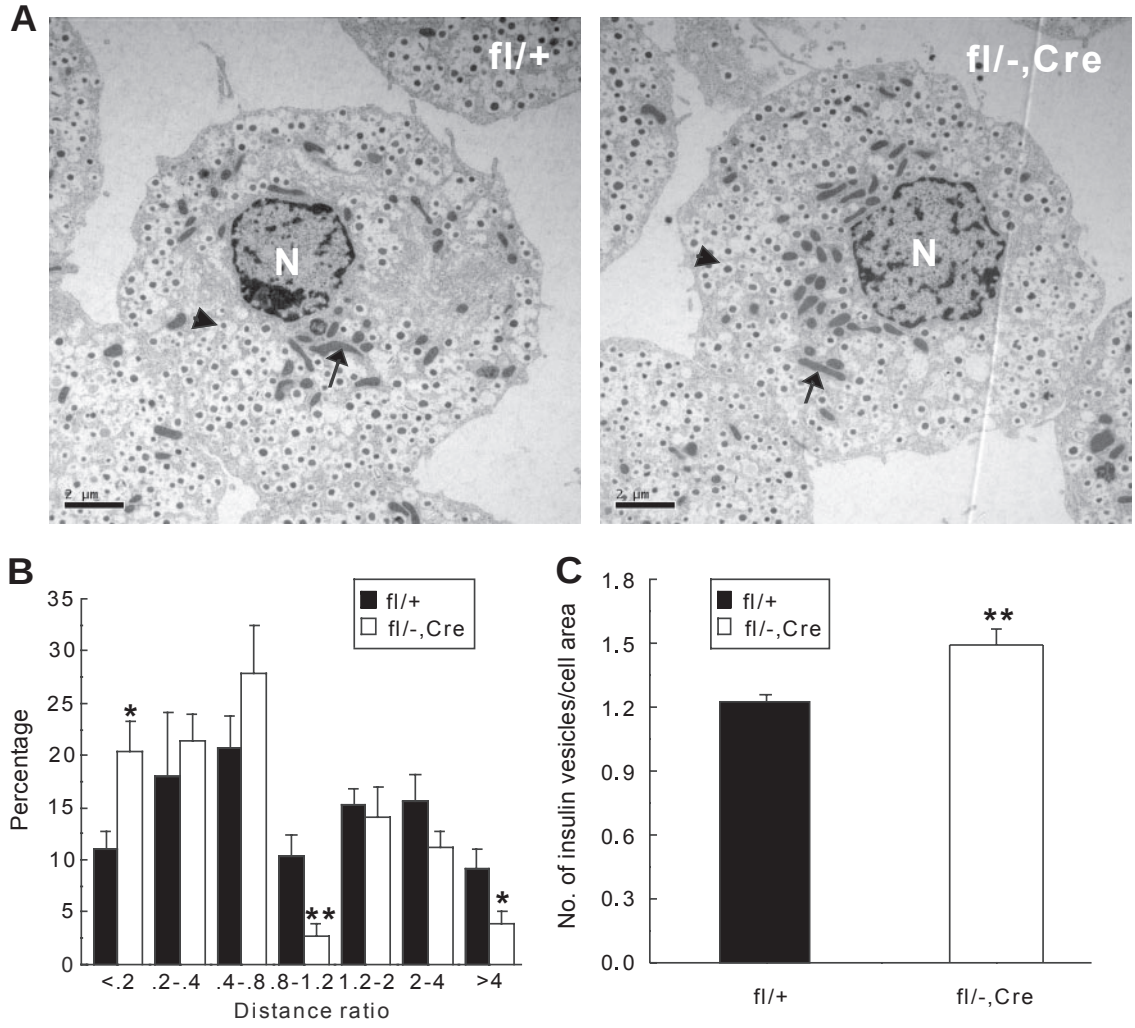

FIG. 7. Ultrastructural insights in pancreatic β-cell based on TEM study. *A*: Representative TEM photos of β-cell from control (*left*) and mutant (*right*) mice. Nuclei (N) were located centrally in both cells. More mitochondria (*arrows*) were located near the nucleus in mutant β-cells. Insulin vesicles (*arrowheads*) were distributed evenly in both mutant and control cells. Scale bar = 2 μm. *B*: Statistical analysis of the distribution of mitochondria in β-cell. The *x*-axis represents the ratio of distances from mitochondria to nucleus and to cell membrane. A ratio <1 indicates that mitochondria are closer to the nucleus, whereas a ratio >1 indicates that mitochondria are closer to the plasma membrane. The *y*-axis represents the percentage of mitochondria in the indicated area. All mitochondria in β-cells are recorded. *C*: Number of insulin vesicles per 1 μm^2 in β-cells. (Fifteen and 26 β-cells are randomly photographed for wild-type and mutant mice, respectively.) *$P < 0.05$, **$P < 0.01$.

islets in these pancreatic specimens showed that the number of islets <4,000 μm^2 was significantly increased in Kif5b conditional knockout mice. However, the number of islets >4,000 μm^2 in mutant mice was comparable to that of wild-type control (Fig. 8*E*). No reduction of islet cell size was observed in Kif5b deficient mice (Fig. 8*F*); therefore, the major factor accounting for reduced islet size was reduced cell number in an islet. We analyzed islet cell proliferation rates in pancreatic sections obtained from 1-month-old mice by BrdU$^+$ labeling. As shown in Figure 8*G*, islet cell proliferation was reduced by ~50% relative to the wild-type control. There was no detectable increase in islet β-cell apoptotic rate based on TUNEL$^+$ analysis (supplementary Fig. 1, available in an online appendix at http://diabetes.diabetesjournals.org/cgi/content/full/db09-1078/DC1).

DISCUSSION

To study the role of Kinesin-1 in pancreatic β-cells in vivo, we have generated cell-specific Kif5b-insKO mice (*Kif5b$^{fl/-}$:RIP2-Cre*) by crossing *Kif5b$^{fl/fl}$* mice with *Kif5b$^{+/-}$:RIP-Cre* mice, in which Cre recombinase is expressed under the control of rat insulin gene promoter (RIP2). Although RIP2-Cre in pancreatic β-cells may have some effect on glucose tolerance in mice (30), this molecular genetic approach allows in vivo studies of specific gene function and could exclude possible side effects of in vitro introduction of anti-kinesin antibodies (33) and overexpression of dominant-negative-acting kinesin (18), which may interfere with biological processes such as endoplasmic reticulum stress.

This in vivo study reveals that Kif5b plays an important role for β-cell function and development. Kif5b-insKO mice displayed significant glucose intolerance and insulin secretory defects. Change in β-cell function was not coupled with changes in islet cell size, islet morphology, and islet cell composition but was associated with a reduced islet size as a consequence of decreased β-cell proliferation rate.

Kif5b-insKO mice exhibited growth retardation within the indicated period. Physiological examination found that Kif5b-insKO mice displayed hyperglycemia and decreased

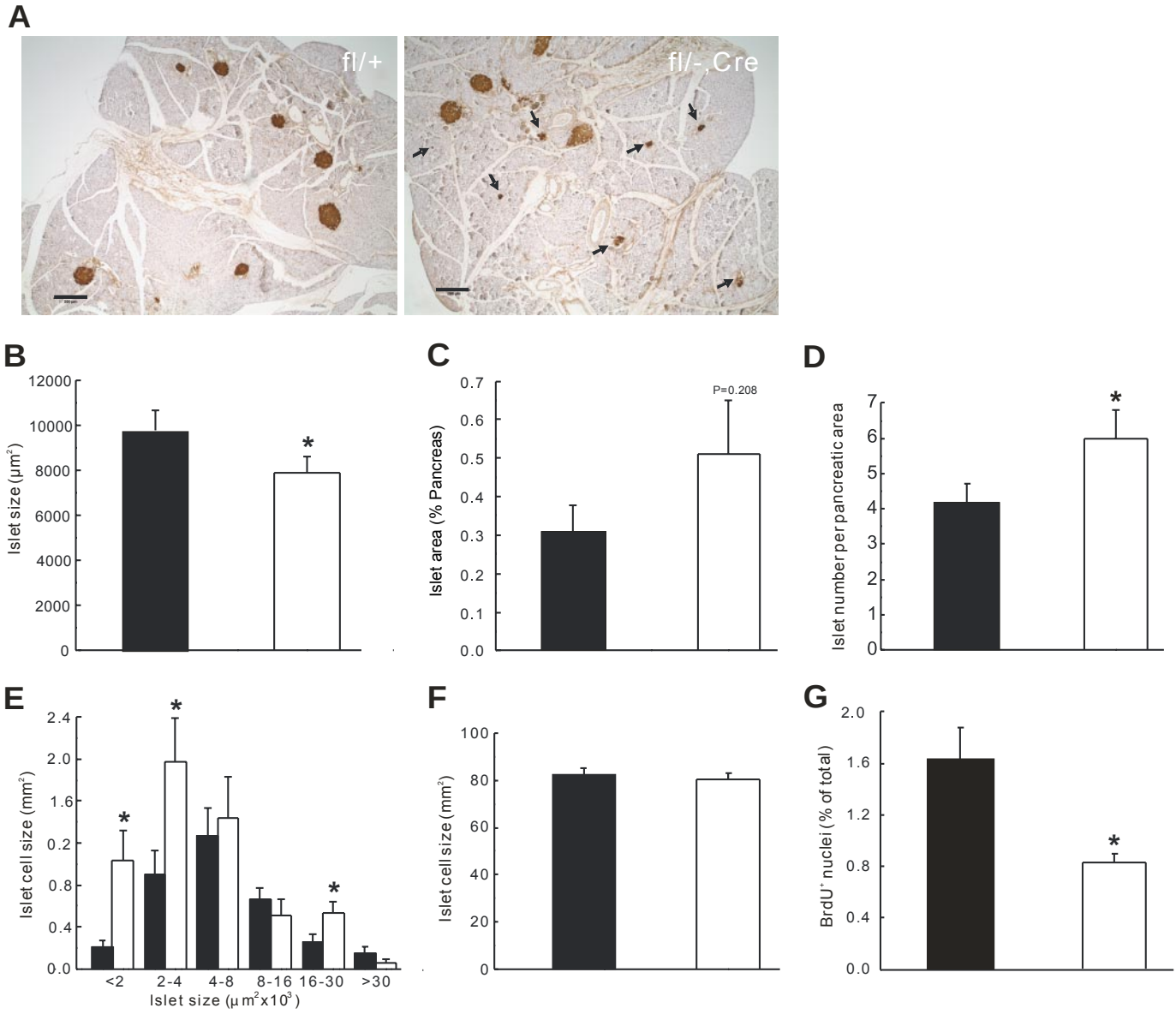

FIG. 8. *Kif5b*$^{fl/-}$*:RIP2-Cre* mice exhibited reduced islet size in pancreas. *A*: Representative microphotographs of pancreatic sections from a control (*left*) and a mutant mouse (*right*) stained by insulin antibody showed the presence of multiples of small islets. *B*: Statistical analysis of the average size of islets in pancreatic samples from control (black bar) and mutant mice (white bar) (all islets in ten whole sections [>300 μm apart] from three wild-type mice and mutant mice were photographed and analyzed). *C*: Total islet area expressed as the percentage of total pancreas area. *D*: Number of islets per 10 mm² of total pancreatic area. *E*: Histomorphometric analysis of the size and number of islets in these pancreatic samples from control and mutant mice. *F*: Mean islet cell size in control and mutant mice. *G*: Frequency of BrdU⁺ staining nuclei in islets as the percentage of total islet nuclei (59 and 62 islets corresponding to three wild-type and three mutant mice, respectively, were imaged and counted). Scale bar = 200 μm. **P* < 0.05. (A high-quality color representation of this figure is available in the online issue.)

plasma insulin levels, together with significantly diminished glucose tolerance and defective insulin secretion, suggesting a role of Kif5b in β-cell function. Our results confirm that Kif5b is required for normal GSIS in an in vivo model. Hypoinsulinemia may account for the poor growth of Kif5b-insKO mice. However, RIP2-Cre expression in hypothalamus and pituitary (24,34) may also lead to the knockout of Kif5b in insulin-positive cells, although no significant reduction of Kif5b level due to Cre expression was observed in hypothalamic lysates of Kif5b-insKO mice. The functions of Kif5b in hypothalamic and pituitary endocrine hormone secretion are unknown at the current stage. Therefore, we cannot rule out the possibility that the observed poor growth is also related to reduced growth hormone and/or insulin-like growth factor secretion.

In vitro studies showed that suppression of Kif5b by overexpression of dominant-negative-acting Kif5b inhibited only the sustained phase of GSIS in clonal β-cells (18). Interestingly, our in vivo GTT results (Fig. 5*A* and *C*) indicated that the defective insulin response to glucose in a Kif5b-insKO mouse occurred in both the early phase and the slow phase. The early phase of insulin secretion is accompanied by Ca^{2+} influx induced exocytosis (1), which requires the metabolism of glucose to create ATP in mitochondria, leading to depolarization of the cell due to the closing of ATP-gated potassium channels. Kif5b and Kif5c have been reported to bind to RanBP2 to determine mitochondria localization and function in neurons (31). In the current study, we found that mitochondria significantly accumulate at the perinuclear region in the β-cell of

Kif5b-insKO mice. Although disruption of Kif5b in extraembryonic cells upregulated the mRNA expression level of Kif5a and Kif5c (32), there is no apparent upregulation of Kif5a/Kif5c at the protein level in mutant β-cells, indicating that Kif5b is the major motor responsible for the dispersion of mitochondria in pancreatic β-cells. The deficiency of mitochondria at the cell peripheral regions may attenuate glucose-to-ATP conversion and partially account for the defect in the early phase of GSIS in response to glucose challenge.

To examine whether blocked Kif5b-mediated insulin vesicle transportation in Kif5b-insKO mice may lead to a decrease in predocked vesicles ready for exocytosis, we also performed TEM studies. However, we observed no significant differences in the number and size of predocked insulin vesicles in Kif5b-insKO mice compared with control mice at the resolution used. Bi et al. (33) observed that KHC (or Kif5b) antibody SUK4 as well as the stalk-tail fragment of KHC specifically inhibited Ca^{2+}-regulated exocytosis in *Lytechinus pictus* sea urchins. Therefore, exocytosis of insulin vesicles could also be affected in the Kif5b knockout islet. In neurons, it was demonstrated that Kif5b can directly bind to syntabulin and SNAP25 to mediate transportation of syntaxin containing vesicles and synaptosome (35,36). Syntaxin and SNAP25 constitute the *t*-SNAREs at the plasma membrane and are functionally required for Ca^{2+}-triggered insulin exocytosis in β-cells (37). *Snap25* mutant mice had impaired insulin granule priming, exocytosis, and recycling in pancreatic β-cells (38). It is possible that knockout of Kif5b in pancreatic β-cells affects the normal distribution and function of the SNARE complex, thereby leading to defects in insulin granule exocytosis. Furthermore, Kif5b functions in several cellular processes including lysosomal distribution and stability in cancer cells and extraembryonic cells (32,39), endoplasmic reticulum to Golgi transportation in Hela cells (40), transportation and axonal targeting of Kv1 channels (41), axonal transport of tubulin heterodimer for microtubule polymerization (42) as well as ribosome translocation (43), etc. Similar cellular functions of Kif5b could occur in pancreatic β-cells. It is tempting to speculate that weakening of both the early and slow phases of insulin response to glucose in Kif5b-insKO mice results from defects in a series of cellular functions after knockout of Kif5b in pancreatic β-cells. Taken together, Kif5b probably exerts a modulatory effect in regulating insulin granule priming and exocytosis in addition to mechanically transporting insulin vesicles. Furthermore, impaired early insulin response is consistent with a defect in glucose tolerance, because the early response is more important for glucose disposal (44). Insulin secretion defects result in a positive feedback for the synthesis of insulin in β-cells, thereby leading to accumulation of insulin in Kif5b-insKO mice islets.

Donelan et al. (45) reported that increased $[Ca^{2+}]_i$ can activate calcineurin in β-granules leading to dephosphorylation of KHC, which is required for transport of β-granules from the storage pool to replenish the readily releasable pool of β-granules. Rab3A is mainly located on the cytosolic face of β-granule membranes. The Rab3A–calmodulin interaction on β-granules is required for activation of calcineurin and dephosphorylation of KHC (46). Yaekura et al. (47) found that knockout of Rab3A in pancreatic β-cells leads to blunted first-phase glucose induced insulin release in vitro and in vivo. Our results together with these studies indicate that any defect of synthesis or dephosphorylation process of KHC can lead to impaired insulin exocytosis.

On the basis of histomorphological investigations, we found a notable increase in the number of small islets in Kif5b-insKO mice (Fig. 8*A* and *E*). $BrdU^+$ staining of 1-month-old mice confirmed that the decreased islet size in Kif5b-inskO mice was due to a defect in islet cell proliferation (Fig. 8*G*). Furthermore, decreased cell proliferation rate was also observed in Kif5b deficient Madin-Darby canine kidney cells (supplementary Fig. 2, available in an online appendix), suggesting that Kif5b plays a conventional role during cell division. Zhu et al. (48) systematically analyzed the functions of all human kinesin/dynein microtubule motor proteins by RNA interference and identified at least 12 human kinesins involved in HeLa cell division. Recently, Haraguchi et al. (49) found that the kinesin-2 complex (KIF3A/3B) is localized with components of the mitotic apparatus such as spindle microtubules and centrosomes and plays an important role not only in interphase but also in mitosis. Both Kif5b and KIF3A/B are microtubule plus end-directed motors for membrane organelle transportation. Therefore, it is of considerable interest to determine whether Kif5b has a similar function or another unique function during cell division.

One seemingly contradictory result found in this study was that islet mass was not affected (Fig. 8*C*) even though β-cell proliferation was inhibited in the Kif5b deficiency mice. Further analysis of the pancreatic sections found that islet number was significantly increased (Fig. 8*D*). Therefore, it is possible that the impaired β-cell function in Kif5b-insKO mice induce β-cell neogenesis to provide a compensatory effect, a process difficult to be defined and more difficult to be quantified at the molecular level (25,50).

In summary, by using Kif5b conditional knockout mice, we have demonstrated that Kif5b is essential in the maintenance of normal β-cell function. Kif5b ablation leads to decreased insulin secretion and diminished glucose tolerance with decreased islet size in the pancreas. Our results indicate that genetic or epigenetic alteration in Kinesin-1 or other related motor proteins may inherit a predisposition to develop diabetes.

ACKNOWLEDGMENTS

This work was supported by grants from the Hong Kong Research Grants Council (RGC) (HKU 7321/04M, HKU 7636/05M) to J.-D.H., a Hong Kong University Small Project Fund to K.-M.Y., and partial funding by an RGC Group Research Project (HKUST6/CRF/08). No potential conflicts of interest relevant to this article were reported.

J.C. wrote the manuscript and researched data. Z.W., Q.C., R.L., and X.-M.Z. researched data. N.G.C. and N.A.J. reviewed/edited the manuscript and generated Kif5b conditional allele. P.S.L. contributed to discussion and reviewed/edited the manuscript. K.-M.Y. and J.-D.H. designed experiments and wrote/reviewed/edited the manuscript.

We thank Dr. Julian Tanner at the University of Hong Kong for his comments on the manuscript.

REFERENCES

1. Safayhi H, Haase H, Kramer U, Bihlmayer A, Roenfeldt M, Ammon HP, Froschmayr M, Cassidy TN, Morano I, Ahlijanian MK, Striessnig J. L-type calcium channels in insulin-secreting cells: biochemical characterization and phosphorylation in RINm5F cells. Mol Endocrinol 1997;11:619–629
2. Wang Z, Oh E, Thurmond DC. Glucose-stimulated Cdc42 signaling is essential for the second phase of insulin secretion. J Biol Chem 2007;282:9536–9546

3. Aguilar-Bryan L, Bryan J. Molecular biology of adenosine triphosphate-sensitive potassium channels. Endocr Rev 1999;20:101–135
4. Kennedy HJ, Pouli AE, Ainscow EK, Jouaville LS, Rizzuto R, Rutter GA. Glucose generates subplasma membrane ATP microdomains in single islet beta-cells. Potential role for strategically located mitochondria. J Biol Chem 1999;274:13281–13291
5. Tsuboi T, McMahon HT, Rutter GA. Mechanisms of dense core vesicle recapture following "kiss and run" ("cavicapture") exocytosis in insulin-secreting cells. J Biol Chem 2004;279:47115–47124
6. Rorsman P, Eliasson L, Renström E, Gromada J, Barg S, Göpel S. The Cell Physiology of Biphasic Insulin Secretion. News Physiol Sci 2000;15:72–77
7. Howell SL, Tyhurst M. Insulin secretion: the effector system. Experientia 1984;40:1098–1105
8. Boyd AE, 3rd, Bolton WE, Brinkley BR. Microtubules and beta cell function: effect of colchicine on microtubules and insulin secretion in vitro by mouse beta cells. J Cell Biol 1982;92:425–434
9. Suprenant KA, Dentler WL. Association between endocrine pancreatic secretory granules and in-vitro-assembled microtubules is dependent upon microtubule-associated proteins. J Cell Biol 1982;93:164–174
10. Hirokawa N, Pfister KK, Yorifuji H, Wagner MC, Brady ST, Bloom GS. Submolecular domains of bovine brain kinesin identified by electron microscopy and monoclonal antibody decoration. Cell 1989;56:867–878
11. Yang JT, Laymon RA, Goldstein LS. A three-domain structure of kinesin heavy chain revealed by DNA sequence and microtubule binding analyses. Cell 1989;56:879–889
12. Yang JT, Saxton WM, Stewart RJ, Raff EC, Goldstein LS. Evidence that the head of kinesin is sufficient for force generation and motility in vitro. Science 1990;249:42–47
13. Xia Ch, Rahman A, Yang Z, Goldstein LS. Chromosomal localization reveals three kinesin heavy chain genes in mouse. Genomics 1998;52:209–213
14. Balczon R, Overstreet KA, Zinkowski RP, Haynes A, Appel M. The identification, purification, and characterization of a pancreatic beta-cell form of the microtubule adenosine triphosphatase kinesin. Endocrinology 1992;131:331–336
15. Batut J, Howell M, Hill CS. Kinesin-mediated transport of Smad2 is required for signaling in response to TGF-beta ligands. Dev Cell 2007;12:261–274
16. Jaulin F, Xue X, Rodriguez-Boulan E, Kreitzer G. Polarization-dependent selective transport to the apical membrane by KIF5B in MDCK cells. Dev Cell 2007;13:511–522
17. Semiz S, Park JG, Nicoloro SM, Furcinitti P, Zhang C, Chawla A, Leszyk J, Czech MP. Conventional kinesin KIF5B mediates insulin-stimulated GLUT4 movements on microtubules. Embo J 2003;22:2387–2399
18. Varadi A, Ainscow EK, Allan VJ, Rutter GA. Involvement of conventional kinesin in glucose-stimulated secretory granule movements and exocytosis in clonal pancreatic beta-cells. J Cell Sci 2002;115:4177–4189
19. Trejo HE, Lecuona E, Grillo D, Szleifer I, Nekrasova OE, Gelfand VI, Sznajder JI. Role of kinesin light chain-2 of kinesin-1 in the traffic of Na,K-ATPase-containing vesicles in alveolar epithelial cells. FASEB J 2010;24:374–382
20. Meng YX, Wilson GW, Avery MC, Varden CH, Balczon R. Suppression of the expression of a pancreatic beta-cell form of the kinesin heavy chain by antisense oligonucleotides inhibits insulin secretion from primary cultures of mouse beta-cells. Endocrinology 1997;138:1979–1987
21. Varadi A, Tsuboi T, Johnson-Cadwell LI, Allan VJ, Rutter GA. Kinesin I and cytoplasmic dynein orchestrate glucose-stimulated insulin-containing vesicle movements in clonal MIN6 beta-cells. Biochem Biophys Res Commun 2003;311:272–282
22. Varadi A, Tsuboi T, Rutter GA. Myosin Va transports dense core secretory vesicles in pancreatic MIN6 beta-cells. Mol Biol Cell 2005;16:2670–2680
23. Rodríguez CI, Buchholz F, Galloway J, Sequerra R, Kasper J, Ayala R, Stewart AF, Dymecki SM. High-efficiency deleter mice show that FLPe is an alternative to Cre-loxP. Nat Genet 2000;25:139–140
24. Gannon M, Shiota C, Postic C, Wright CV, Magnuson M. Analysis of the Cre-mediated recombination driven by rat insulin promoter in embryonic and adult mouse pancreas. Genesis 2000;26:139–142
25. Roccisana J, Reddy V, Vasavada RC, Gonzalez-Pertusa JA, Magnuson MA, Garcia-Ocaña A. Targeted inactivation of hepatocyte growth factor receptor c-met in beta-cells leads to defective insulin secretion and GLUT-2 downregulation without alteration of beta-cell mass. Diabetes 2005;54:2090–2102
26. Postic C, Shiota M, Niswender KD, Jetton TL, Chen Y, Moates JM, Shelton KD, Lindner J, Cherrington AD, Magnuson MA. Dual roles for glucokinase in glucose homeostasis as determined by liver and pancreatic beta cell-specific gene knock-outs using Cre recombinase. J Biol Chem 1999; 274:305–315
27. Kulkarni RN, Brüning JC, Winnay JN, Postic C, Magnuson MA, Kahn CR. Tissue-specific knockout of the insulin receptor in pancreatic beta cells creates an insulin secretory defect similar to that in type 2 diabetes. Cell 1999;96:329–339
28. Silva JP, Köhler M, Graff C, Oldfors A, Magnuson MA, Berggren PO, Larsson NG. Impaired insulin secretion and beta-cell loss in tissue-specific knockout mice with mitochondrial diabetes. Nat Genet 2000;26:336–340
29. Kanai Y, Okada Y, Tanaka Y, Harada A, Terada S, Hirokawa N. KIF5C, a novel neuronal kinesin enriched in motor neurons. J Neurosci 2000;20:6374–6384
30. Lee JY, Ristow M, Lin X, White MF, Magnuson MA, Hennighausen L. RIP-Cre revisited, evidence for impairments of pancreatic beta-cell function. J Biol Chem 2006;281:2649–2653
31. Cho KI, Cai Y, Yi H, Yeh A, Aslanukov A, Ferreira PA. Association of the kinesin-binding domain of RanBP2 to KIF5B and KIF5C determines mitochondria localization and function. Traffic 2007;8:1722–1735
32. Tanaka Y, Kanai Y, Okada Y, Nonaka S, Takeda S, Harada A, Hirokawa N. Targeted disruption of mouse conventional kinesin heavy chain, kif5B, results in abnormal perinuclear clustering of mitochondria. Cell 1998;93:1147–1158
33. Bi GQ, Morris RL, Liao G, Alderton JM, Scholey JM, Steinhardt RA. Kinesin- and myosin-driven steps of vesicle recruitment for Ca2+-regulated exocytosis. J Cell Biol 1997;138:999–1008
34. Biondi CA, Gartside MG, Waring P, Loffler KA, Stark MS, Magnuson MA, Kay GF, Hayward NK. Conditional inactivation of the MEN1 gene leads to pancreatic and pituitary tumorigenesis but does not affect normal development of these tissues. Mol Cell Biol 2004;24:3125–3131
35. Su Q, Cai Q, Gerwin C, Smith CL, Sheng ZH. Syntabulin is a microtubule-associated protein implicated in syntaxin transport in neurons. Nat Cell Biol 2004;6:941–953
36. Diefenbach RJ, Diefenbach E, Douglas MW, Cunningham AL. The heavy chain of conventional kinesin interacts with the SNARE proteins SNAP25 and SNAP23. Biochemistry 2002;41:14906–14915
37. Easom RA. Beta-granule transport and exocytosis. Semin Cell Dev Biol 2000;11:253–266
38. Jeans AF, Oliver PL, Johnson R, Capogna M, Vikman J, Molnár Z, Babbs A, Partridge CJ, Salehi A, Bengtsson M, Eliasson L, Rorsman P, Davies KE. A dominant mutation in Snap25 causes impaired vesicle trafficking, sensorimotor gating, and ataxia in the blind-drunk mouse. Proc Natl Acad Sci U S A 2007;104:2431–2436
39. Cardoso CM, Groth-Pedersen L, Høyer-Hansen M, Kirkegaard T, Corcelle E, Andersen JS, Jäättelä M, Nylandsted J. Depletion of kinesin 5B affects lysosomal distribution and stability and induces peri-nuclear accumulation of autophagosomes in cancer cells. PLoS One 2009;4:e4424
40. Gupta V, Palmer KJ, Spence P, Hudson A, Stephens DJ. Kinesin-1 (uKHC/KIF5B) is required for bidirectional motility of ER exit sites and efficient ER-to-Golgi transport. Traffic 2008;9:1850–1866
41. Rivera J, Chu PJ, Lewis TL, Jr, Arnold DB. The role of Kif5B in axonal localization of Kv1 K(+) channels. Eur J Neurosci 2007;25:136–146
42. Kimura T, Watanabe H, Iwamatsu A, Kaibuchi K. Tubulin and CRMP-2 complex is transported via Kinesin-1. J Neurochem 2005;93:1371–1382
43. Diefenbach RJ, Diefenbach E, Douglas MW, Cunningham AL. The ribosome receptor, p180, interacts with kinesin heavy chain, KIF5B. Biochem Biophys Res Commun 2004;319:987–992
44. Del Prato S, Tiengo A. The importance of first-phase insulin secretion: implications for the therapy of type 2 diabetes mellitus. Diabetes Metab Res Rev 2001;17:164–174
45. Donelan MJ, Morfini G, Julyan R, Sommers S, Hays L, Kajio H, Briaud I, Easom RA, Molkentin JD, Brady ST, Rhodes CJ. Ca2+-dependent dephosphorylation of kinesin heavy chain on beta-granules in pancreatic beta-cells. Implications for regulated beta-granule transport and insulin exocytosis. J Biol Chem 2002;277:24232–24242
46. Kajio H, Olszewski S, Rosner PJ, Donelan MJ, Geoghegan KF, Rhodes CJ. A low-affinity Ca2+-dependent association of calmodulin with the Rab3A effector domain inversely correlates with insulin exocytosis. Diabetes 2001;50:2029–2039
47. Yaekura K, Julyan R, Wicksteed BL, Hays LB, Alarcon C, Baskin D, Poitout V, Philipson LH, Rhodes CJ. Rab3A null mice develop a pancreatic β-cell defect glucose intolerance due to an insulin exocytotic defect. Diabetes 2002;51(Suppl. 2):A72
48. Zhu C, Zhao J, Bibikova M, Leverson JD, Bossy-Wetzel E, Fan JB, Abraham RT, Jiang W. Functional analysis of human microtubule-based motor proteins, the kinesins and dyneins, in mitosis/cytokinesis using RNA interference. Mol Biol Cell 2005;16:3187–3199
49. Haraguchi K, Hayashi T, Jimbo T, Yamamoto T, Akiyama T. Role of the kinesin-2 family protein, KIF3, during mitosis. J Biol Chem 2006;281:4094–4099
50. Bernal-Mizrachi E, Wen W, Stahlhut S, Welling CM, Permutt MA. Islet beta cell expression of constitutively active Akt1/PKB alpha induces striking hypertrophy, hyperplasia, and hyperinsulinemia. J Clin Invest 2001;108:1631–1638